

AD-A040 613

NORTHWESTERN UNIV EVANSTON ILL DEPT OF MATERIALS SCIENCE F/G 20/11  
COMPARISON OF STRESS MEASUREMENTS BY X-RAYS WITH THREE DIFFERENT--ETC(U)  
MAY 77 M R JAMES, J B COHEN

N00014-75-C-0580

UNCLASSIFIED

TR-17

NL

1 OF 1  
ADA  
040613



END

DATE  
FILMED  
7-77

AD A 040613

# NORTHWESTERN UNIVERSITY

## DEPARTMENT OF MATERIALS SCIENCE

Technical Report No. 17  
May 20, 1977

Office of Naval Research  
Contract N00014-75-C-0580  
NR 031-733

COMPARISON OF STRESS MEASUREMENTS BY X-RAYS WITH THREE DIFFERENT DETECTORS  
AND A STRONGLY FLUORESCING SPECIMEN

by

M. R. James and J. B. Cohen

Distribution of this Document  
is Unlimited.

Reproduction in whole or  
in part is permitted for  
any purpose of the United  
States Government.



EVANSTON, ILLINOIS

AD No. \_\_\_\_\_  
DDC FILE COPY



COMPARISON OF STRESS MEASUREMENTS BY X-RAYS WITH THREE DIFFERENT DETECTORS  
AND A STRONGLY FLUORESCING SPECIMEN

M. R. James and J. B. Cohen

Northwestern University

Evanston, Illinois 60201

ABSTRACT

Measurements on the heat affected zone of a weldment are presented using the position sensitive detector and a normal diffractometer equipped with a scintillation detector and a solid state detector. The sample, a surface ground titanium alloy, provided a classic applications problem for the X-ray technique from which a real analysis of the position sensitive detector could be made. The diffraction profile from the Ti alloy is very broad and the fluorescence produces a high background. The fluorescence is easily rejected using a solid state detector, however, the time of analysis is very long. With the position sensitive detector, the combination of increased energy discrimination over the scintillation detector and the simultaneous measurement of many data points over the broad peak enabled the measurements to be made for the same accuracy in much shorter times than for either the solid state detector or the scintillation detector.

REVISION 1st	
NTIS	White Section <input checked="" type="checkbox"/>
DOC	Buff Section <input type="checkbox"/>
UNANNOUNCED	<input type="checkbox"/>
JUSTIFICATION	
BY	
DISTRIBUTION/AVAILABILITY CODES	
DISL	AVAIL. INFO. SPECIAL
A	

## CHAPTER 6\*

## 6.1 INTRODUCTION

The residual stress distribution near a fillet weld joining two titanium alloy plates was examined by means of X-rays. Titanium is a difficult material in which to measure the residual state by the X-ray technique because fluorescence and broadening of the diffraction profile makes accurate peak location difficult. This sample presents a classic application problem and thereby allows a realistic comparison to be made between a scintillation detector, a solid state detector (SSD) and a position sensitive detector (PSD) in the measurement of residual stress. The SSD has the advantage of excellent energy resolution which enables the fluorescence to be removed to improve the diffraction profile.

At the Naval Shipyards, two titanium plates, 12.7 x 10.2 x 2.5 cm, had been surface ground and welded at right angles along the long dimension. As shown in Fig. 6.1, a photograph of the sample, the plates were cut apart away from the weld. The residual stress distribution was measured in the heat affected zone near the weld. A timing comparison between the three detectors revealed the PSD to be faster than either of the other detectors.

Using the PSD, the distribution of residual stresses in the heat affected zone was determined. Residual stresses were measured in both the transverse and parallel directions with respect to the bead. The distribution is compared with theoretical predictions for typical stress distributions after welding. The predictions assume the stress

---

\* Chs. 1-3 constitute TR No. 14, Ch. 4 is TR No. 16, and Ch. 5 is TR No. 15.

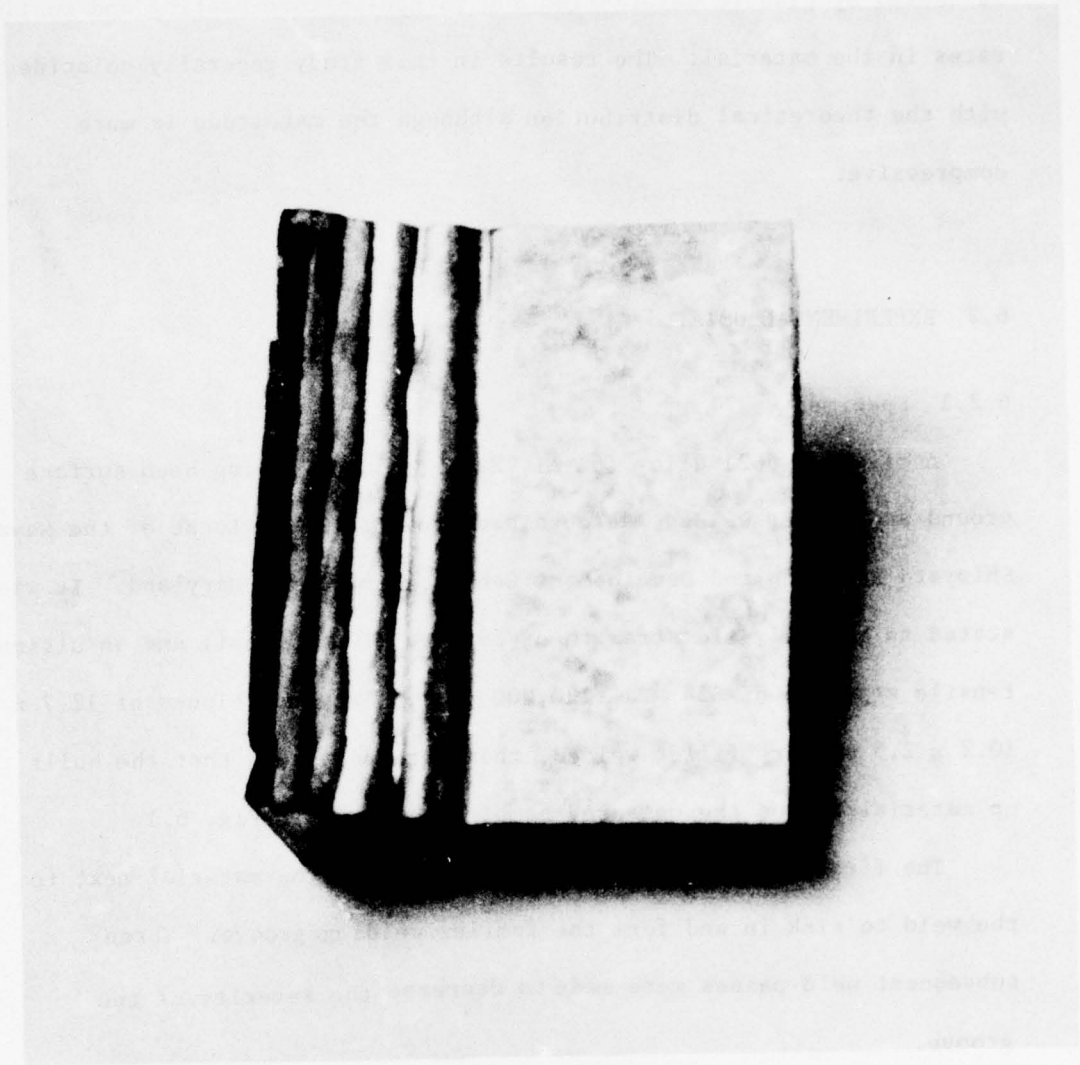


FIGURE 6.1 Photograph of the Ti alloy specimen having been fillet welded using a multipass method. The saw grooves on the left side can be seen where the second block, located at right angles to the sample in the picture, had been cut away for convenience. The residual stress distribution was measured on the flat portion of the sample.



is caused by plastic deformation due to non-uniform heating and cooling rates in the material. The results in this study generally coincide with the theoretical distribution although the magnitude is more compressive.

## 6.2 EXPERIMENTAL DETAILS

### 6.2.1 Specimen

A titanium #621 alloy (6% Al, 2% Nb, 1% Ni) having been surface ground and fillet welded was obtained from Dr. W. H. Lucke of the Naval Shipyard Research and Development Center, Annapolis, Maryland. It was stated to have a yield strength of 695 MPa (100,000 psi) and an ultimate tensile strength of 834 MPa (120,000 psi). Two such blocks of 12.7 x 10.2 x 2.5 cm were fillet welded, then cut apart such that the built up material was on the measured sample, as shown in Fig. 6.1.

The first welding pass causes the edges of the material next to the weld to sink in and form the familiar welding groove. Three subsequent weld passes were made to decrease the severity of the groove.

Typical mechanical properties for a 6% Al, 4% V titanium alloy are  $E = 110 \text{ GPa}$  ( $16 \times 10^6 \text{ psi}$ ) and  $\nu = .34$ .<sup>(93)</sup> The X-ray elastic constants for this alloy have been measured previously for the 114 planes using  $\text{Cu}_{K\alpha}$  radiation.<sup>(94,95)</sup> The reported X-ray elastic constants give a value for  $E/(1+\nu)$  of 64.6 GPa ( $9.3 \times 10^6 \text{ psi}$ ). This is 20 pct smaller than the value calculated from bulk mechanical values. The studies conducted in this section were made using a stress constant of 335 MPa/ $^{\circ}2\theta$

(48000 psi/ $^{\circ}2\theta$ ) for the 114 planes using  $\text{Co}_{K\alpha}$  radiation. This value was obtained using the measured X-ray elastic constants from ref. 94.

#### 6.2.2 Data Collection

Complete automation of the residual stress measurement was accomplished using the computer package (ONR TR No. 16). A Picker diffractometer was utilized with a scintillation detector, solid state detector (SSD) and a position sensitive detector (PSD). The  $\sin^2\psi$  method was used for measurements with the scintillation detector and the SSD using inclinations of  $0^{\circ}$ ,  $26.57^{\circ}$ ,  $39.23^{\circ}$  and  $50.72^{\circ}$  and five data points to locate the peak position. Background subtraction was used in determining the region of fit for the scintillation detector because the peak to background ratio was only 1.2 due to the poor energy discrimination. The correlation coefficient for  $d$  vs.  $\sin^2\psi$  was always greater than .97 indicating a linear relationship to a 99 pct confidence level.

The two tilt technique could be used with the PSD because  $d$  vs.  $\sin^2\psi$  was linear. The collection of many data points on the peak minimizes the random errors as shown in ONR TR No. 14 so the use of the two tilt technique using the PSD is as accurate as the  $\sin^2\psi$  technique using the other two detectors since  $d$  vs.  $\sin^2\psi$  was linear. Calibration of the PSD was accomplished using three low order peaks.

The position of the 010 ( $41.053^{\circ}2\theta$ ), 002 ( $44.820^{\circ}2\theta$ ) and 011 ( $47.053^{\circ}2\theta$ ) peaks were found using the program ALIGN with a solid state detector. The PSD was then mounted with the  $2\theta$  arm of the Picker diffractometer set to  $44.00^{\circ}2\theta$  and the peak location for all three peaks determined simultaneously.

This gave a calibration constant of  $.0405^\circ 2\theta/\text{channel}$ . The residual stress measurements were made with the  $2\theta$  arm set to  $154.00^\circ 2\theta$  when using the PSD.

A Co tube operated at 50 kV and 6 mA was used on the Picker diffractometer with a divergent slit of  $2^\circ$ . For the scintillation detector and the SSD a  $.2^\circ$  receiving slit was used. In all cases the pulse height analyzer was set at 90% of the  $\text{Co}_{K\alpha}$  radiation.

### 6.3 TIMING COMPARISON

The stress,  $\sigma_x$ , was measured at point A in the center of the sample as shown in Fig. 6.2 using three detectors. A statistical counting error of  $\pm 14$  MPa ( $\pm 2030$  psi) was specified and the results are given in Table 6.1.

The profile at  $\psi=0^\circ$  is shown in Fig. 6.3 for the scintillation detector and the SSD and in Fig. 6.4 for the PSD. It can be seen that the profile is better characterized with the SSD in that the peak is sharper and has a better peak to background ratio than for the other detectors because the Ti fluorescence is eliminated. However, the intensity is considerably decreased so that more time is spent in the preliminary scans.

The PSD is seen to be the fastest method as expected. For the scintillation detector, the automated program had great difficulty finding the peak because of the poor peak to background ratio. This was not the case with the PSD since the energy resolution is 20%<sup>\*</sup>

---

\*The resolution is given as a ratio of the full width at half maximum intensity of the energy peak to the mean energy expressed as a percentage.



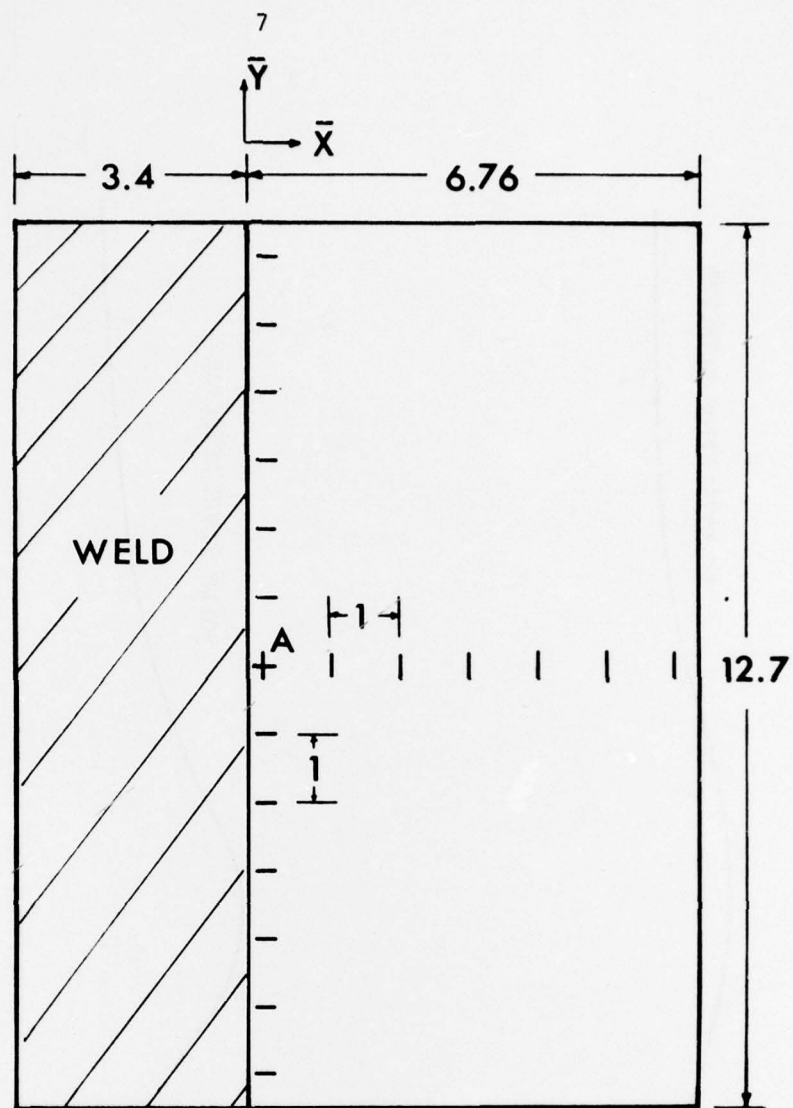


FIGURE 6.2 Location of stress measurements on Ti alloy specimen. Measurements along the line parallel to the weld give  $\sigma_x$  and measurements transverse to the weld give  $\sigma_y$ . Distances in cm.

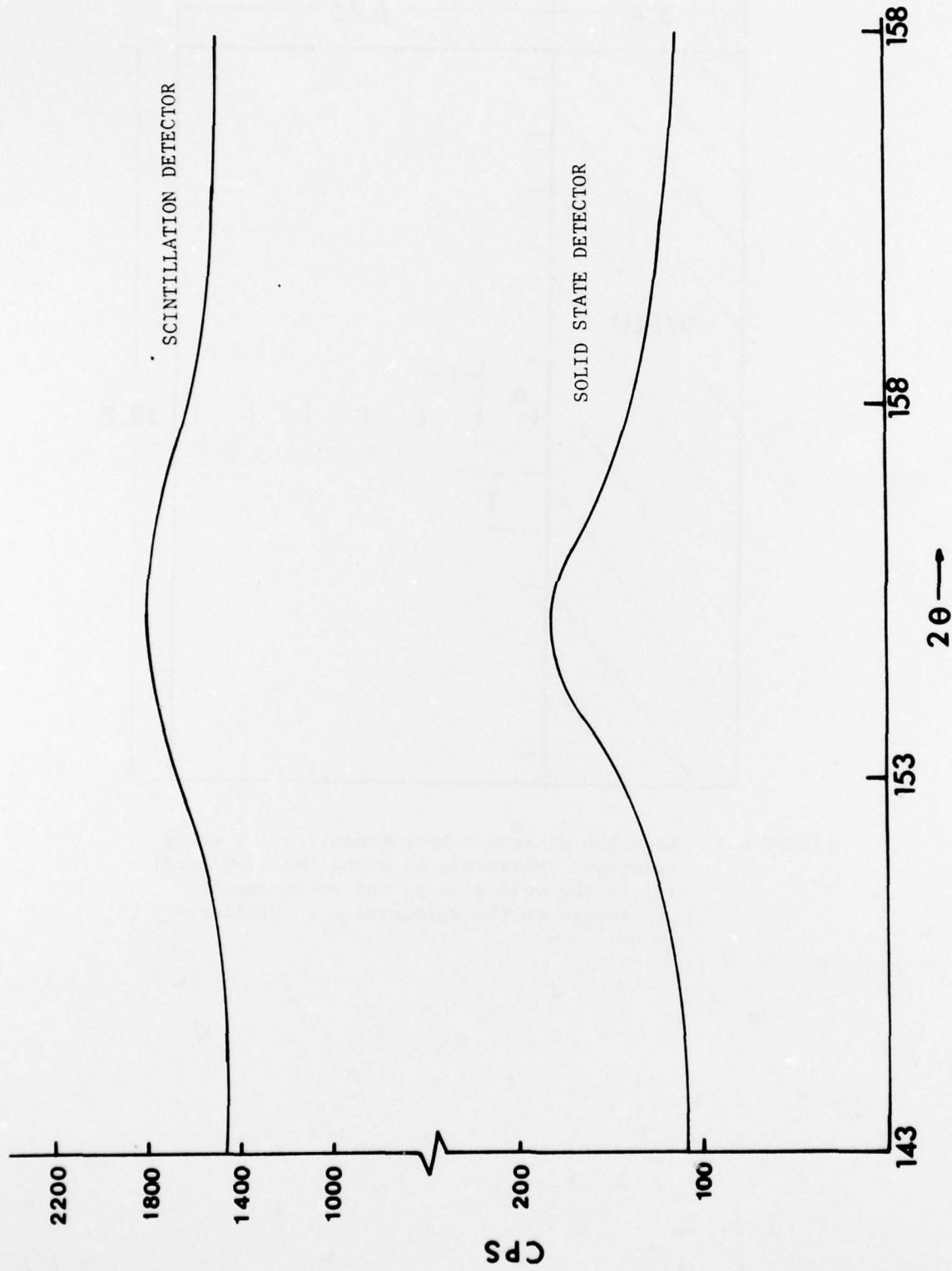


FIGURE 6.3 Diffraction profile for Ti alloy. 114 peak,  $\text{CoK}\alpha$  radiation.

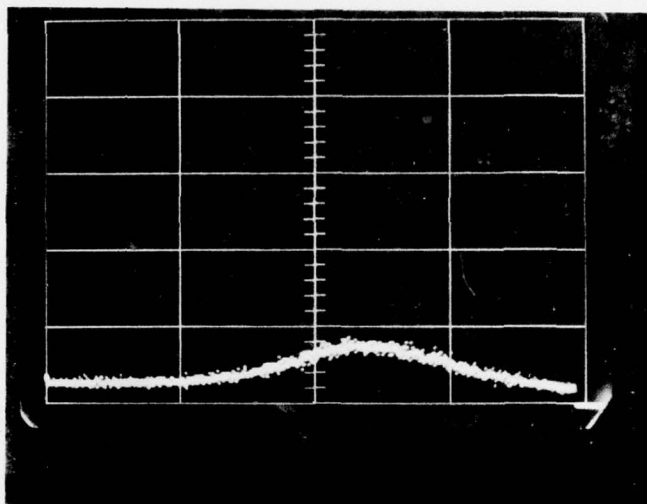


FIGURE 6.4 Diffraction profile for the Ti alloy sample using the position sensitive detector. 114 peak,  $\text{CoK}\alpha$ .

TABLE 6.1  
 DETECTOR COMPARISON  
 STRESS,  $\sigma_x$ , MEASURED AT POINT A IN FIG. 6.2

Detector	Stress MPa (psi)	Error MPa (psi)	Time Minutes
PSD	-351.2 (-50931)	$\pm 16.3$ ( $\pm 2360$ )	2
SCINTILLATION	-363.4 (-52710)	$\pm 17.3$ ( $\pm 2515$ )	25
SSD	-333.6 (-48379)	$\pm 14.7$ ( $\pm 2140$ )	30

PSD - Two tilt method.

SCINTILLATION -  $\sin^2\psi$  method with background subtraction.

SSD -  $\sin^2\psi$  method.



compared to 50% for the scintillation detector so that some of the fluorescence could be eliminated.

#### 6.4 STRESS DISTRIBUTION IN THE HEAT AFFECTED ZONE

The residual stress distribution was measured in the heat affected zone near the weld using the PSD. With the coordinate system in Fig. 6.2, the residual stresses parallel to the weld bead,  $\sigma_y$ , were measured along a line perpendicular to the weld and the stress,  $\sigma_x$ , was measured along a line parallel to the bead. The results are plotted in Fig. 6.5 for  $\sigma_y$  and Fig. 6.6 for  $\sigma_x$ .

In welding operations involving any of the various titanium alloys, the fusion zone and part of the heat affected zone are heated to temperatures within the  $\beta$  phase (BCC) field and on completion of the welding cycle cool back through the  $\beta$  transition temperature to the  $\alpha$  phase (HCP). For the titanium alloy in this study, the transformation product on cooling is a supersaturated martensitic  $\alpha$  having limited quantities of Nb and Ni held mainly in solid solution.<sup>(96)</sup> A review of the causes of residual stress formation is presented to explain the distribution.

Nagaraja and Tall<sup>(97)</sup> suggest that many factors influence the residual stress distribution because the stresses are produced by plastic flow caused by non-uniform heating of the material. These factors include the geometry of the plates, type and heat of welding, speed of welding and the rate of cooling as well as the physical properties of the metal and make it difficult to predict the distribution. Masubuchi<sup>(98)</sup> claims the basic distribution is most influenced by the thermal process of contraction and the plastic deformation.

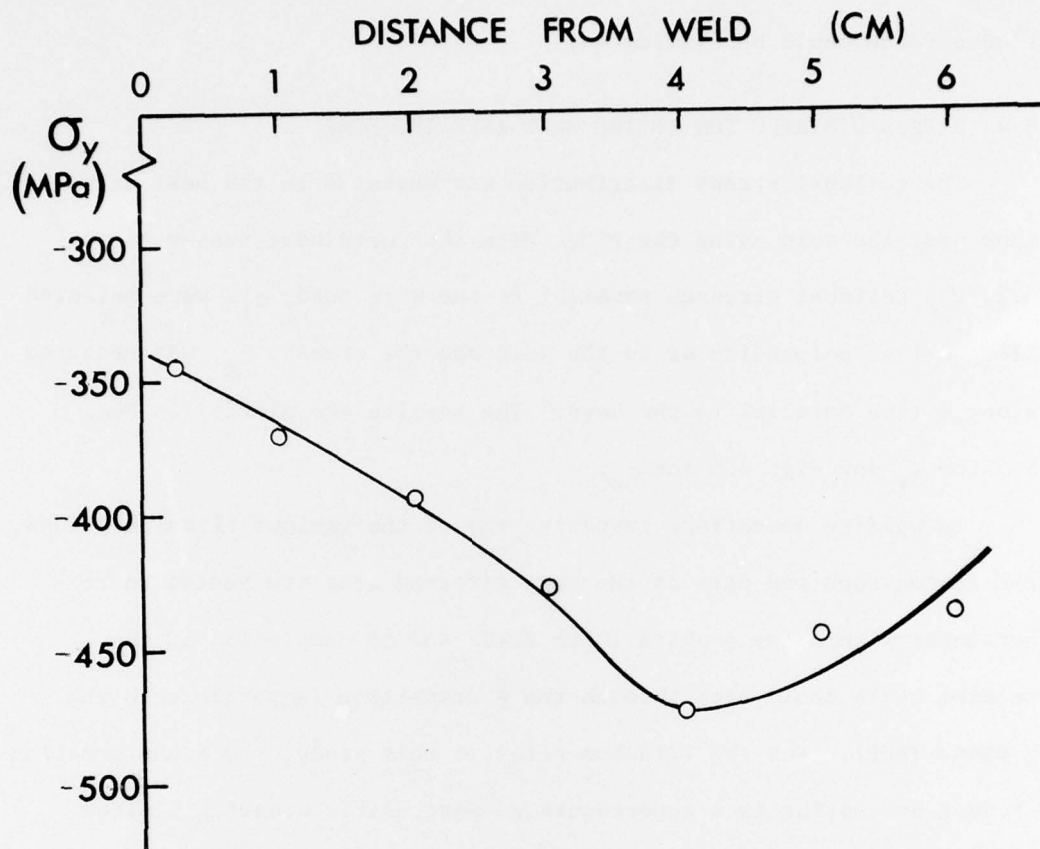


FIGURE 6.5 Stress distribution for  $\sigma_y$  transverse to weld bead.

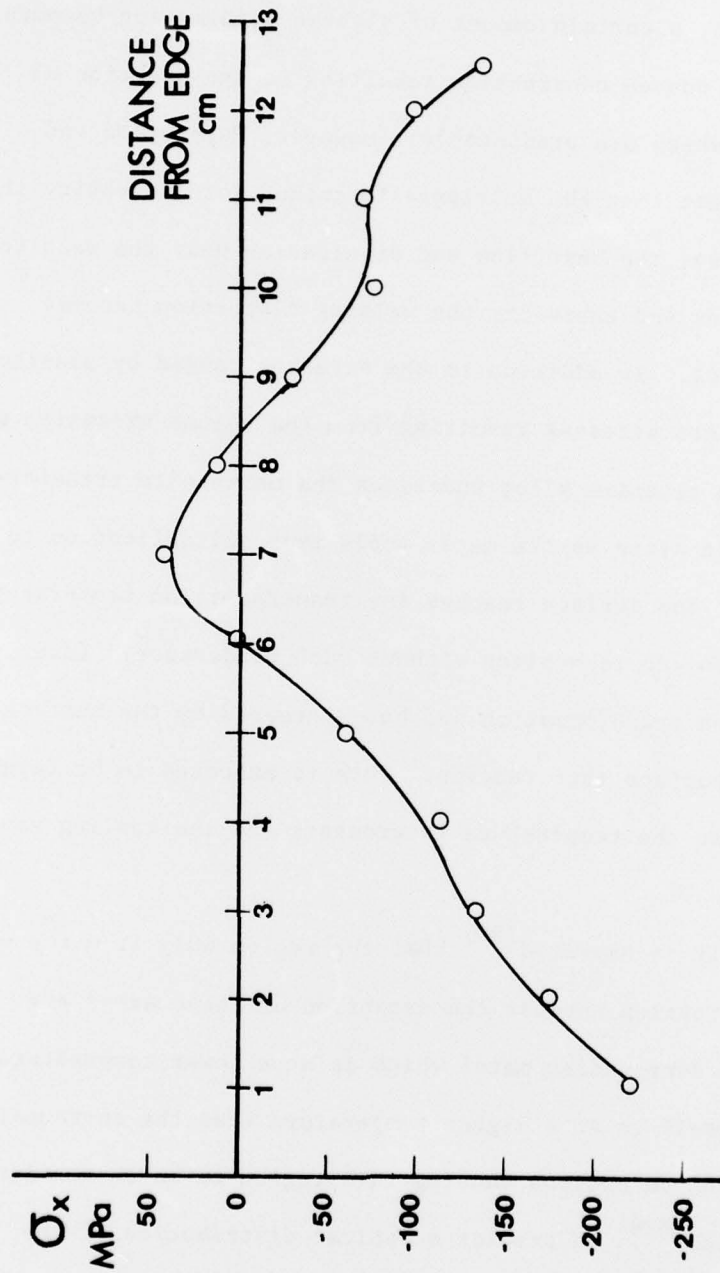


FIGURE 6.6 Stress distribution for  $\sigma_x$  parallel to weld bead.

The plastic deformation occurs because the cooler surrounding metal hinders expansion of the molten metal in all directions except on the surface. Here displacement of metal occurs and when that region cools and contracts, a certain amount of plastic deformation becomes permanent, causing uneven contraction resulting in the creation of residual stresses which are predictable. However, Papazoglou and Masubuchi<sup>(99)</sup> suggest that the multipass technique for decreasing the welding groove causes the heat flow and dissipation near the weld to be extremely complex and therefore the welding distortion becomes difficult to predict. In addition to the stresses caused by plastic deformation there are stresses resulting from the volume expansion which takes place as the titanium alloy undergoes the martensite transformation in the solid state as the metal cools from solidification to room temperature. The surface reaches the transformation temperature first and expansion can take place without much hinderance. Later, the bulk will expand on transformation and be compressed by the surface, thus driving the surface into tension. This is expected to be largest near the weld where the temperature is greatest and the cooling rate fastest.

In general, it is expected<sup>(99)</sup> that the region away from the weld should be in compression because the expansion of these areas are restrained by the surrounding metal which is at a lower temperature. The weld metal itself is at a higher temperature than the surroundings and tends to shrink on cooling causing this region to be in tension. This leads Masubuchi<sup>(98)</sup> to predict a typical distribution of the residual stresses in a butt weld as shown in Fig. 6.7.



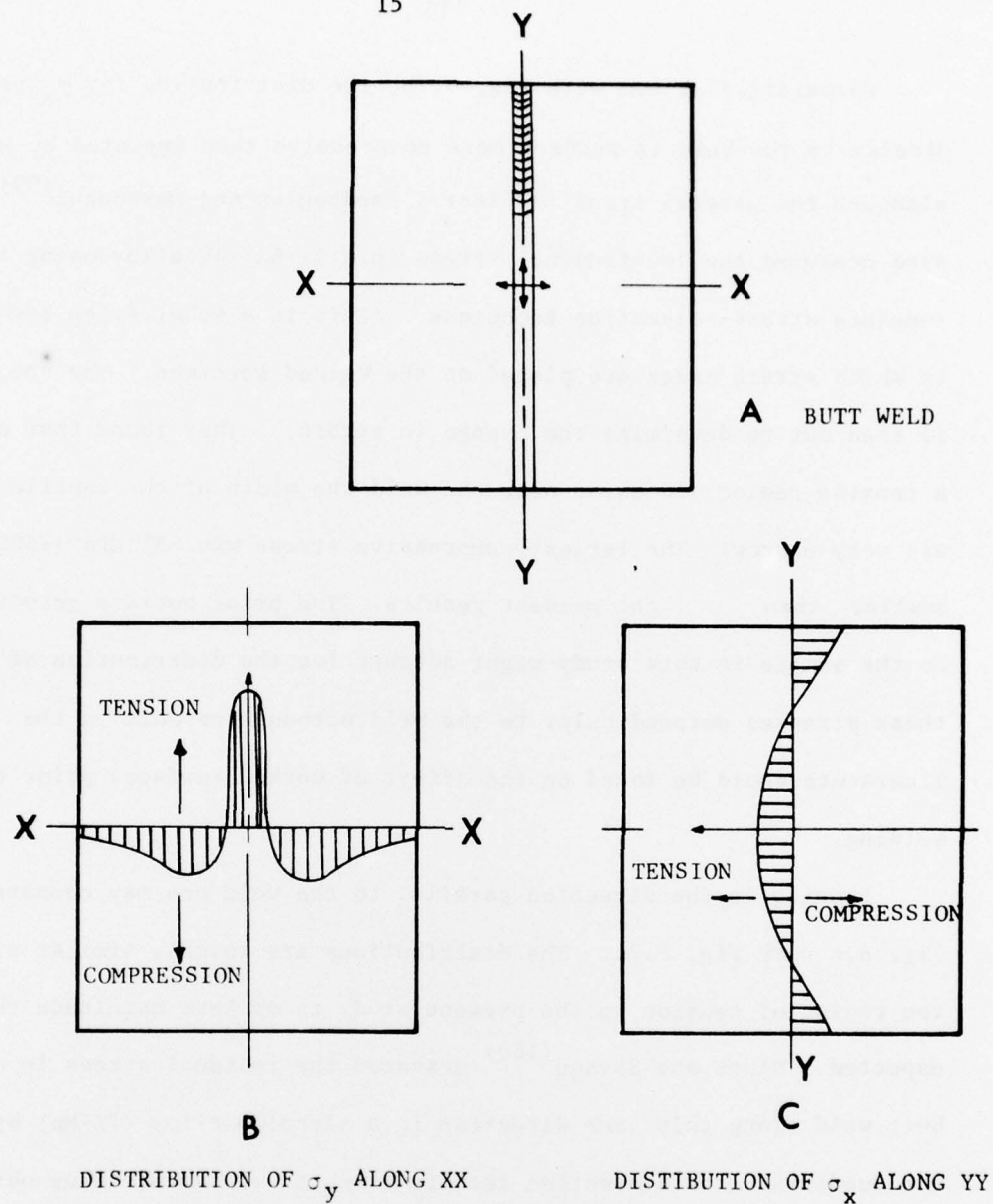


FIGURE 6.7 Typical distributions of residual stresses in a butt weld.  
From reference 98.

Comparing Fig. 6.5 with Fig. 6.7b, the distribution for  $\sigma_x$  perpendicular to the bead is perhaps more compressive than expected by Masubuchi although the general trend is clear. Papazoglou and Masubuchi<sup>(99)</sup> also measured the longitudinal stress in a Ti-6Al-4V alloy using the complete stress-relaxation technique. (This is a subdivision technique in which strain gages are placed on the welded specimen. The specimen is then cut to determine the change in strain.) They found that although a tensile region did exist near the weld the width of the tensile zone was very narrow. The largest compressive stress was -35 MPa (-5000 psi), smaller than the present results. The prior surface grinding on the sample in this study might account for the distribution of these stresses perpendicular to the weld although no work in the literature could be found on the affect of worked surfaces prior to welding.

Looking in the direction parallel to the weld one may compare Fig. 6.6 with Fig. 6.7c. The distributions are roughly similar although the region of tension in the present study is of less magnitude than expected. Nipes and Savage<sup>(100)</sup> measured the residual stress in a butt weld along this same direction in a titanium alloy (7%-Mn) by the subdivision or dissection technique mentioned above. They obtained compressive weld stresses in the transverse direction,  $\sigma_x$ , along most of the weld although the magnitude (less than -70 MPa) was not as great as in this study. They showed that the magnitude of the stresses depends on the size of the plate as expected since this influences the cooling rates. The general distribution is, however, not affected. The results presented here are therefore consistent.

## 6.5 SUMMARY

It was shown quite conclusively that the PSD was capable of being used to measure the residual stress in less time than a SSD or a scintillation detector. The entire stress distribution was determined in less than 2 hours using the PSD and is reasonably consistent with theoretical predictions given all the variables that may change the stress state. This type of analysis would have been very time consuming (~ 15 hours) with either of the other detectors.

## REFERENCES

93. F. A. McClintock and A. S. Argon, Mechanical Behavior of Materials, Addison-Wesley Publ. Co., Reading, MA. (1966).
94. A. L. Esquivel, Adv. in X-Ray Analysis, 12, 269 (1969).
95. B. Singh, D. Lewis and J. R. Lee, Proc. 3rd Int. Conf. Nondes. Test., 743 (1961), Tokyo, Japan.
96. R. E. Goosey, in Heat-Treatment Aspects of Metal Joining Processes, The Iron and Steel Institute (1972) p. 61.
97. N. R. Nagaraja Rao and L. Tall, The Welding Journal, 40, Research Supplement, 468-S, (1961).
98. K. Masubuchi, in Weld Imperfections: Proc. of a Sym. at Lockheed, Palo Alto Research Lab., Addison-Wesley Publ. Co., (1966) p. 567.
99. V. Papazoglou and K. Masubuchi, ONR Contract No. N00014-75-C-0469, NR 031-773, Sept. 1976.
100. E. F. Nipes and W. F. Savage, Welding Research, 37, Research Supplement 133-S, (1958).



Unclassified

Security Classification

DOCUMENT CONTROL DATA - R & D

(Security classification of title, body of abstract and indexing annotation must be entered when the overall report is classified)

1. ORIGINATING ACTIVITY (Corporate author)		2a. REPORT SECURITY CLASSIFICATION	
J. B. Cohen, Northwestern University, Evanston, IL		Unclassified	
		2b. GROUP	
3. REPORT TITLE			
COMPARISON OF STRESS MEASUREMENTS BY X-RAYS WITH THREE DIFFERENT DETECTORS AND A STRONGLY FLUORESCING SPECIMEN			
4. DESCRIPTIVE NOTES (Type of report and inclusive dates)			
Technical Report, No. 17			
5. AUTHOR(S) (First name, middle initial, last name)			
M. R. James and J. B. Cohen			
6. REPORT DATE		7a. TOTAL NO. OF PAGES	7b. NO. OF REFS
N00014-75-C-0580 NR 031-733		18	8
8a. CONTRACT OR GRANT NO.		9a. ORIGINATOR'S REPORT NUMBER(S)	
5345-455		Technical Report No. 17	
b. PROJECT NO.		9b. OTHER REPORT NO(S) (Any other numbers that may be assigned this report)	
c. 11 20 May 77		None	
10. DISTRIBUTION STATEMENT			
Distribution of this document is unlimited.			
11. SUPPLEMENTARY NOTES		12. SPONSORING MILITARY ACTIVITY	
		Office of Naval Research Metallurgy Branch	
13. ABSTRACT			
<p>Measurements on the heat affected zone of a weldment are presented using the position sensitive detector and a normal diffractometer equipped with a scintillation detector and a solid state detector. The sample, a surface ground titanium alloy, provided a classic applications problem for the X-ray technique from which a real analysis of the position sensitive detector could be made. The diffraction profile from the Ti alloy is very broad and the fluorescence produces a high background. The fluorescence is easily rejected using a solid state detector, however, the time of analysis is very long. With the position sensitive detector, the combination of increased energy discrimination over the scintillation detector and the simultaneous measurement of many data points over the broad peak enabled the measurements to be made for the same accuracy in much shorter times than for either the solid state detector or the scintillation detector.</p>			

DD FORM 1473

1 NOV 65

(PAGE 1)

S/N 0101-807-6801

Unclassified

Security Classification

260810

JB

